

Original Article

Experimental Investigation on Similar and Dissimilar Materials of AZ31/AZ91 Mg Alloys by Friction Stir Welding

M. Yugandhar¹, B. Prabhakar Kammar², S. Nallusamy³

¹Department of Mechanical Engineering, Research Center-New Horizon College of Engineering, Bengaluru, India.

²Department of Mechanical Engineering, Gopalan College of Engineering and Management, Bengaluru, India.

³Department of Adult, Continuing Education and Extension, Jadavpur University, Kolkata, India.

¹Corresponding Author : yugandhar077@gmail.com

Received: 18 August 2022

Revised: 20 October 2022

Accepted: 02 November 2022

Published: 26 November 2022

Abstract - Friction Stir Welding (FSW) efficiently bonded with two exceptional magnesium (Mg) plates one with less aluminum (AZ31/AZ91) content as well as the opposite with more aluminum (AZ91/AZ31). The impact of procedure elements on warm crack improvement was tested. In most efficient procedure situations at one-of-a-kind parameters (AZ91/AZ91 and AZ31/AZ31 comparable aggregate) with one-of-a-kind rpm like 1600, 1400, and 1200 and one-of-a-kind feed charges like 25,50 and 75mm/min feed under this sound weld 1400 rpm with 25 mm/min feed. A valid metallurgical joint with great grains and dispersed (Mg17Al12) phase inside the nugget zone become achieved and parallel (AZ31/AZ91 multiple mixtures). A growing fashion in hardness measures has also revealed the extended aluminum dissolution in the nugget region. The AZ31 Mg alloy aspect (advancing) had a distinct touch between the nugget sector and the Thermo Mechanical Affected Quarter (TMAZ), but no longer the AZ91 Mg alloy side (withdrawing). It is viable to draw conclusions based on the findings. FSW can be used to sign up for assorted metals, including difficult-to-method metals like Mg alloys, and warm cracking may cause completely prevented by deciding on suitable system parameters to gain a sound joint. The impact of manner optimizing values for the joining of AZ91/AZ31 Mg alloy plates at some point of FSW became investigated in this observation. A hit joint was installed at a device circular motion of 1100rpm and also a device journey space of 25mm/min. The aggregate for holder along with tool rotational and travel speeds has had a large impact on the fabric waft tactics in the nugget region. The microstructural analyses revealed that the joint improvement changed in most cases as a result of the mechanical blending of the additives. The nugget sector changed discovered to be terrible, and there has been a sharp interface on the joint. Microhardness assessments throughout the weld joint adding indicated a lack of entire metallurgical bonding. The presence of magnesium and aluminum turned into revealed by way of X-ray diffraction material examination on the weld area. From the observed results, it may be concluded that FSP may be used to combine AZ91 Mg alloy and AZ31 alloy despite the fact that complex demanding situations in fabric blending require additional exploration.

Keywords - Similar, Dissimilar, AZ-31/AZ91, FSW process, Nugget zone, Thermo mechanical, HAZ, TAMZ.

1. Introduction

The ability to form permanent bonds between dissimilar metals is essential to the advancement of high-performance lightweight systems with improved gas performance in automotive programs. On the other hand, combining incompatible metals using a phase of solid-state welding practices is technologically demanding in fabrication shops [1]. Non-ferrous metal systems such as aluminum (Al) alloys and also magnesium (Mg) alloys were so much recognized and widely used in structural applications. Today's layout and manufacturing business have ever-increasing requirements for connecting dissimilar metals. In this regard, combining two non-ferrous metals expands the range of utilization within manufacturing trading companies. It is difficult to register different alloys in the same base material [2]. Welding of compatible alloys

is particularly complex when simple materials such as Al-Mg, Al-steel, and Mg-steel are chemically unique [3, 4]. The melting coefficient, heat transfer charge, temperature-related plastically phase change, and amorphous crystal structure for the basic materials were the most influential facts that made it as difficult as nature to incorporate liquid lands in Al and Mg alloys [5, 6].

Table 1. Material composition

Material	% of Elements Weight							
	Mg	L	N	I	N	R	Ferrous	O
AZ31	96.54	2.34	0.63	0.005	0.19	0.00	0.01	0.00
AZ91	89	8.3	0.35	0.00	0.00	0.00	0.00	0.00

Alternatively, the FSW process a powerful technique developed for joining dissimilar sheets not melting as per shapes was becoming increasingly common like a solid-



phase joining of steels. Most of the Mg-based diverse welding research work has been done using one of the Mg alloys in the AZ collection as the base material. An AZ31-Mg alloy to a zinc-coated low-carbon metal was effectively bonded, with the appearance of low-melting-point eutectic segments that allow greater diffusion between the magnesium alloys and reported that it was created as a result of steel together [7]. Magnesium alloy AZ91, which he modified to Al_3Mg_2 , was mixed with embedded eutectic of Mg and $Mg_{17}Al_{12}$, and the lap shear force of the joint changed to AZ31 magnesium alloy on the right alloy [8].

Conshohocken [9] refers to the formation of intermetallic layers of his $Mg_{17}Al_{12}$ and Al_3Mg_2 within the multi-welded region of Al-5083 and AZ31 alloys effectively welded sheets of AA-5754 and AZ31 and found that have stress, ductility stages of the mate parts were reduced comparing at underlying material for total process parameters [10, 11]. Figure 1 shows that an AZ31-Mg alloy sheet is attached to his 1060 Al alloy and observed a touch with a lamellar structure. Additionally, a centerline break within the weld joint was found due to the generation of Al_3Mg_2 and $Al_{12}Mg_{17}$ steps within the weld region found similar brittle fractures in AZ31-O welded joints. FSW Advanced Mg alloy due to the critical mixing of soil materials in the stirring area. It is also observed that the tensile energy of sweat tissue is reduced compared to each basic substance [12].

Intermetallic compounds (between Mg and Al) are formed at certain stages during the mating of AZ91 alloy to less carbon steel also AM60 Mg composition into DP600 second-segment steel [13]. In the old painting, FSW successfully joined AZ31/ AZ91 Mg alloy, but galvanic corrosion reduced the corrosion performance of the joints [14]. As previously mentioned, the mechanical mixing of dissimilar metals is an important mechanism for forming bond fabrics with and without a base layer [15, 16].

However, there is insufficient information in the literature regarding the mating of AZ91 Mg and AZ-31 alloy. As a result, FSW used AZ91magnesiumalloy and AZ31magnesiumalloy for fasteners in this study. Several combinations of fixture rotation speed and tool travel speed were used to achieve a good bond. The essential factors determining fabric flow in welds of various sheets of steel were studied through microstructure examination and also micro Vickers hardness measurements at the mating joints. The literature on mating AZ91-Mg / AZ-31 alloys is incomplete. As a final result, in modern research FSW used his AZ91 and AZ31 magnesium alloys for fastening. Various examinations of tool circular motion and also fixture circular rotation were used to obtain high-quality joints. The key factors that determine material flow in characteristic metal welds have been studied by micro-structural observation and microhardness measurements in welded joints.

2. Experimental Work

Figure 2 shows the Vertical or Horizontal setup by Kitamura has the five-Axis machining solution to give you the aggressive area needed to system all your complex, multi-sided elements in a single set-up. Kitamura's Trunnion desk design gives the users elevated accuracy and rigidity, simple set-up, and simplicity of programming for the operator, and permits for max stiffness and versatility with the ability to put the painting piece toward the spindle. 4+1 or full simultaneous control, our five-axis line-up has you blanketed. For the trials, sheets of the alloys AZ91 Mg (specific Magnesium, Hyderabad, India) and A31 (NUFIT PIPING answers) measuring 100x50x6mm each were fabricated the idea substances chemicals are indicated on the desk.

The portions of labor were placed on the work surface as shown in Figures 2, 3, 4, 5 and 6. Snapshots showing (a) the components of the paintings make-up on the work surface of the FSW tool and (b) the popular milling machine that was emphasized in this work. A trendy-motive CNC milling gadget (Kitamura) and an FSW device produced through FSW turned into utilized to complete the operation composed of 15mm shoulder diameter H13 tool steel, a pin with a five-1mm taper, and a 4mm distance.



Fig. 1 Vertical machining centre



Fig. 2 Experimental setup (Kitamura X2 Mycentre)

Figure 1 displays an image of the gear and FSW system that has been utilized in this investigation. It became welded using distinctive device (1200, 1400, 1600, and 1800 rpm) rotational prices and distance (25, 50, and 75mm/min) speeds. The technique specs had been chosen

based totally on the literature and thinking of the gadget's available speed and feed changes out the tests [17]. The weld joint becomes d and analyzed for each mixture of processing parameters. At 1200rpm, a hit joint without becoming produced 25mm in keeping with minute feed 30x10x6 mm every combination of 6 specimens was sliced throughout the microstructural investigations and the welding route has been achieved [18]. The samples had been initially polished with the use of various specimens like comparable and numerous AZ31 and AZ91 Alloys (1200rpm with 25mm/min, 50mm/min, 75mm/min traverse speed we applied) similar to 1400mm rpm and 1600rpm with similar mating and assorted mating alloys callously made 18 combinations.

Use sandpaper grades were at 2000 grit, usual at clay form sharpening. These samples are well-polished. Using a wheel polisher and diamond paste after each step, use ethanol to loosen the sample very well and dispose of any leftovers from the forecasting grinding step. Chemical etching reagents are also used to take picric acid reagents and optical microscopy pictures with polished samples. Germany). When measuring hardness (Omnitech, India), his three samples of 50x30x4mm were cut across the weld. Measurements were taken at a period of 0.5mm, so the ground structure, Heat Affect Zone (HAZ), thermodynamic nuzzet zone then auto-affected zone TMAZ is measured. The weight of 185gms along with in dwell time of 15 seconds was used for the measurements. X-ray diffraction studied (XRD, Baruker Advances D8, USA) is performed on base metals, welded joints, etc. A scan from 25° to 88° [19] with a step length of 0.1° for CuK emission was achieved.

2.1. Selection of Work Pieces

- a) AZ-91:- A block like 350x45x55mm -1 nos. This we cut by using a metal cutter into a different sizes like 10x55x10mm-28 nos. Again use a milling machine to make the piece like 50x100x6.00(+0.1)
- b) Az-31:-Directly buy material like 50x100x6.00 (+0.1)
- c) Cool selection:-I buy a raw material H13 tool steel like dia25x150-4 NOS

AISI H13 metal is a 5% Cr metal alloy with high molybdenum and vanadium content for ultra-high performance equipment. Molybdenum imparts excellent durability and excessive hardening. Vanadium enhances the dispersion of difficult vanadium carbides and increases toughness. H13 Device Metal is a hardened metal [20]. It has moderate tempering resistance, moderate thermal fatigue resistance, and excellent hot cracking resistance while retaining excessive hardness and performance at improved temperatures. It is a deep cure, has fully expanded toughness, and can be air-cooled to cure large areas. It is also resistant to thermal fatigue, erosion, and delamination making it suitable for a variety of high-temperature applications. Ideal as a moulded cover for aluminum die casting and magnesium die casting as shown in Figure 3. However, H13 metal is susceptible to hydrogen embrittlement and can be nitride to increase tarnish resistance.

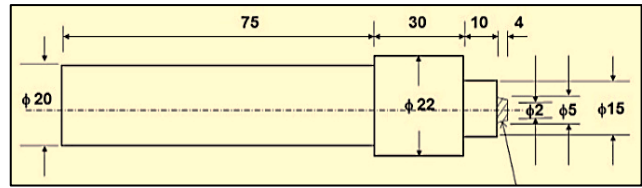


Fig. 3 H-13 Tool steel material

2.2. Experimental Process

2.2.1. Similar butt joint with metal process parameters (AZ-31)/ 25 Tool traverse Speed (TTS)

In AZ31 similar to butt welding at 25 tool traverse speed, the weld was made at different RPMs, here as per my experimental work we used here CNC-vertical milling machine, a tool was tapered threaded at 4.3mm length will go between the two metals showing in Figure 4(a), 4(b) and 4(c). AISI H13 metal is a 5% Cr metal alloy with high molybdenum and vanadium content for ultra-high performance equipment [21]. Molybdenum imparts excellent durability and excessive hardening.

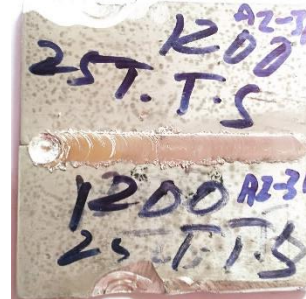


Fig. 4a The weld made at 1200rpm at 25 tool traverse speed with similar welding Az31 alloy

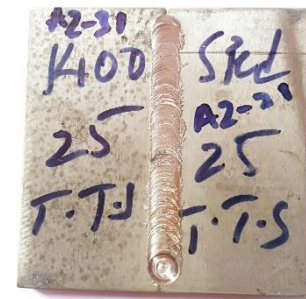


Fig. 4b The weld was made at 1400rpm at 25 tool traverse speed with similar welding Az31 alloy

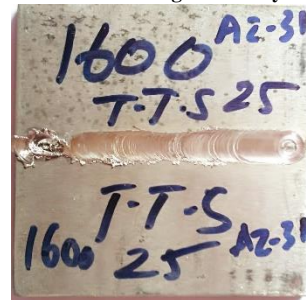


Fig. 4c The weld made at 1600rpm at 25 tool traverse speed with similar welding Az31 alloy

Vanadium enhances the dispersion of difficult vanadium carbides and increases toughness. H13 device metal is a hardened metal. It has moderate tempering resistance, moderate thermal fatigue resistance, and excellent hot cracking resistance while retaining excessive hardness and performance at improved temperatures [22]. It

is a deep cure, has fully expanded toughness, and can be air-cooled to cure large areas. It is also resistant to thermal fatigue, erosion, and delamination making it suitable for a variety of high-temperature applications.

Ideal as a moulded cover for aluminum die casting and magnesium die casting. However, H13 metal is susceptible to hydrogen embrittlement and can be nitride to increase tarnish resistance. And the width will be at the top point tool shoulder the width of the butt weld is 5mm and the depth point bottom it touches with a 2mm tip and the shoulder to endpoint the length was 4.3mm, but here we use the material thickness was 6.1 to 6.3mm because we need to achieve the proper welding. FSW is currently used to successfully consolidate sheets of AZ31 Mg alloy.

Achieving a robust weld between two similar metals is highly dependent on the speed of rotation [48] and the travel of the tool. The tool circular orientation of 1200rpm, 1400rpm, and 1600rpm along with a tool traverse speed of 25mm/minute were determined to be suitable settings for an FSW fixture along with a shoulder diameter of 15mm, a tape pin of 5 to 2mm, also the length of 4.35mm. We found that the bonding between AZ31-Mg and AZ31 alloys is often the result of mechanical intermixing and weak metallurgical bonding.

The stirred quarter region and the AZ31 similar matrix had a sharp interface according to microstructural observations and microhardness studies. Furthermore, it was found that the second phase of AZ31-Mg [24] alloy faded and the particles of the stirrer became smaller. No significant new values were found in the XRD analysis after FSW. Initial results suggest similar studies to determine the effects of the presence of various metals in welded joints from the mechanical and corrosive behavior of joints. Using AZ31 Mg FSW and additional studies on mechanical performance, corrosion range, and AZ-31 base fabric, it is clear that the alloy was AZ31 alloy plates were joined.

Moreover, it was noted that the second segment of AZ31-Mg alloy also small size grains decreased from the stir region. In this case, no significant found values were found in the XRD analysis after FSW [25]. Additional research is to determine the impact of using non-identical metals. It is proposed to evaluate how the participation of dissimilar materials at the mating parts affects the mechanical then corrosion properties of the joint.

Table. 2 Machining process is done as per the step by step

S. No	RPM/Tool Travel Speed	25 (TTS)	50 (TTS)
1	1200	ok	ok
2	1400	ok	ok
3	1600	ok	ok

3. Experiment setup with Results and Discussions

3.1. Similar butt Joint with Metal Process Parameters (AZ-31)/ 50 Tool Traverse Speed (TTS)

In AZ31 similar to butt welding at 50 tool traverse speed, the weld was made at different RPMs, here as per my

experimental work we used here CNC-vertical milling machine, and a tool was tapered threaded at 4.3mm length will go between the two metals, and the width will be at the top point, tool shoulder the width of butt weld is 5mm and the depth point bottom it touches with 2mm tip and the shoulder to endpoint the length was 4.3 mm [26], but here we use the material thickness was 6.1 to 6.3mm because we need to achieve the proper welding. FSW is currently used successfully as shown in Figures 5(a), 5(b) and 5(c) consolidate sheets of AZ31 Mg alloy.



Fig. 5a The weld made at 1200rpm at 50 tool traverse speed with similar welding Az31 alloy

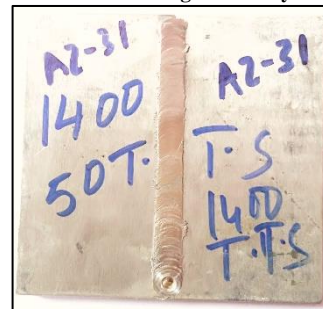


Fig. 5b The weld was made at 1400rpm at 50 tool traverse speed with similar welding Az31 alloy

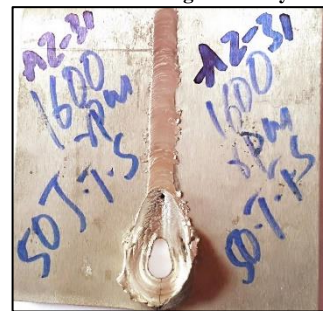


Fig. 5c The weld was made at 1600rpm at 50 tool traverse speed with similar welding Az31 alloy

3.2. Similar butt Joint with Metal Process Parameters (AZ-91)

3.2.1 Similar butt Joint with Metal Process Parameters (AZ-91) / 25 Tool Traverse Speed (TTS)

In AZ91 similar butt welding at 25 tool traverse speed, the weld was made at different rpm here as per my experimental work we used here CNC -Vertical Milling Machine, a tool was tapered threaded at 4.3mm length will go between the two metals and the width will be at the top point that is tool shoulder the width of butt weld is 5mm and the depth point bottom it touches with 2mm tip and the shoulder to endpoint the length was 4.3 mm as shown in Figures 6(a), 6(b) and 6(c). But here we use the material

thickness was 6.1 to 6.3mm because we need to achieve the proper welding.

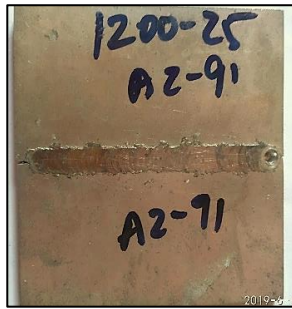


Fig. 6a The weld made at 1200rpm at 25 tool traverse speed with similar welding Az91 alloy

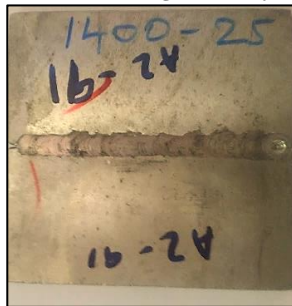


Fig. 6b The weld was made at 1400rpm at 25 tool traverse speed with similar welding Az91 alloy



Fig. 6c The weld was made at 1600rpm at 25 tool traverse speed with similar welding Az91 alloy

Friction stir welding is currently used to successfully consolidate sheets of AZ31 Mg alloy. Achieving a robust weld between two similar metals has been found to be highly dependent on the speed of circular motion, and traverse of the tool. A tool circular motion speed of 1200,1400, and1600 rpm, and a tool traverse speed of 50 mm/min were determined to be suitable settings for an FSW fixture, as also a shoulder diameter of 16mm, a tapered from5 to 2 mm of pin size, also a length up to 4.3mm.

We found that the bonding between AZ31-Mg and AZ31 alloys is often the result of mechanical intermixing and weak metallurgical bonding. The stirred quarter region and the AZ31 similar matrix had a sharp interface according to microstructural observations and microhardness studies. Furthermore, it was found that the second phase of AZ31-Mg alloy faded and the particles of the stirrer became smaller. No significant new values were found in the XRD analysis after FSW.

Initial results suggest similar studies to determine the effects of the presence of various metals in welded joints from mechanical, corrosive behavior from joints. Using

AZ31 Mg FSW and additional studies on mechanical performance, corrosion range, and AZ-31 base fabric, it is clear that the composition of AZ31composition sheets can be mated. Moreover, it was noted that the second segment of AZ31-Mg alloy with low-size grains decreased at the stirring point. Not a significant enrich value is found in the XRD analysis after FSW [30-32]. Additional research is to determine the impact of using non-identical metals. It is proposed to evaluate how the supervision of non-similar metals in the mating affects the mechanical and corrosion properties at the joint.

3.2.2 Similar butt Joint with Metal Process Parameters (AZ-91)/ 50 Tool Traverse Speed (TTS)

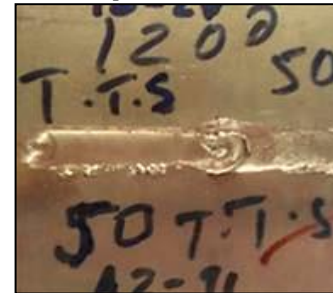


Fig. 7a The weld made at 1200rpm at 50 tool traverse speed with similar welding Az91 alloy



Fig. 7b The weld was made at 1400rpm at 50 tool traverse speed within stir welding Az91 alloy



Fig. 7c The weld was made at 1600rpm at 50 tool traverse speed with similar welding Az91 alloy

AZ91 is similar to butt welding at 50 tool traverse speed, the weld was made at different rpm, here as per my experimental work we used here CNC -vertical milling machine, a tool was tapered threaded at 4.3mm length will go between the two metals and the width will be at the top point, tool shoulder the width of butt weld is 5mm and the depth point bottom it touches with 2mm tip and the shoulder [33] to endpoint the length was 4.3 mm but here we use the material thickness was 6.1 to 6.3mm because we need to achieve the proper welding as shown in Figures 7(a), 7(b) and 7(c).

The stirred quarter region and the AZ91 similar matrix had a sharp interface according to microstructural observations and microhardness studies. Furthermore, it was found that the second phase of AZ91-Mg alloy faded and the particles of the stirrer became smaller. No significant new values were found in the XRD [34] analysis after FSW. Initial results suggest similar studies to determine the effects of the presence of various metals in welded joints on the mechanical and corrosive behavior of the joints.

Using AZ91 Mg FSW and additional studies on mechanical performance corrosion range, and AZ-91 base fabric, it is clear that the alloy and AZ91 alloy sheets can be joined [35]. Moreover, it was noted that the second segment of AZ91-Mg alloy with smaller grains decreased in the stir region. No significant new values were found in the XRD analysis after FSW. Additional research is to determine the impact of using non-identical metals. It is proposed to evaluate how the presence of dissimilar metals in the welded joint affected mechanical, and corrosion properties for similar and non-similar mating.

3.3. Dissimilar butt Joint with Metal Process Parameters (AZ-91/AZ-31)

3.3.1. Similar butt Joint with Metal Process Parameters (AZ-91/31)/ 25 Tool Traverse Speed (TTS)

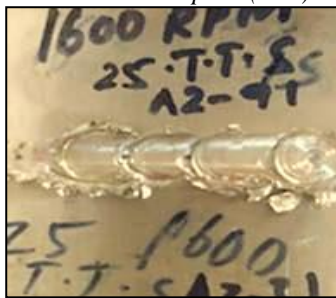


Fig. 8a The weld made at 1200rpm at 25 tool traverse speed with Dissimilar welding Az91/Az31 alloy



Fig. 8b The weld was made at 1400rpm at 25 tool traverse speed with dissimilar welding Az91/Az31 alloy

In AZ31/AZ91 Dissimilar butt welding at 25 tool traverse speed, the weld was made at different rpm as shown in Figures 8(a) and 8(b) here as per my experimental work. The CNC-vertical milling machine was used here, a tool was tapered and threaded at a 4.3mm length will go between the two metals and the width will be at the top point of is tool's shoulder the width of the butt weld is 5mm and the depth point bottom it touches with 2mm tip and the shoulder to endpoint the length was 4.3 mm, but here we use the

material thickness was 6.1 to 6.3mm because we need to achieve the proper welding.

FSW is currently used to successfully consolidate sheets of AZ91 Mg alloy and AZ31 alloy. Achieving a robust weld between two dissimilar metals has been found to be highly dependent on the different speeds. We found that the bonding between AZ91-Mg and AZ31 alloys is often the result of mechanical intermixing and weak metallurgical bonding. The stirred quarter region and the AZ91 matrix had a sharp interface according to microstructural observations and microhardness studies. Furthermore, it was found that the second phase of AZ91-Mg alloy faded and the particles [36] of the stirrer became smaller. No significant new values were found in the XRD analysis after FSW. Initial results suggest similar studies to determine the effects of the presence of various metals in welded joints on the mechanical and corrosive behavior of the joints. Using AZ91 Mg FSW and additional studies on mechanical performance, corrosion range, and AZ-31 base fabric, it is clear that the alloy and AZ 31 alloy sheets can be joined. Moreover, it was noted that the second segment of AZ91-Mg alloy with smaller grains decreased in the stir region.

No significant new values were found in the XRD analysis after FSW. Additional research is to determine the impact of using non-identical metals. It is proposed to evaluate how the presence of dissimilar metals in the welded joint affects the mechanical and corrosion properties of the joint. Here using SEM Analysis we found some mechanical failures and other analytical things under the retreating and advancing zones. The basic microstructure of magnesium alloy AZ91 consists of a primary α -phase with an aluminium-rich β -phase (Mg 17 Al 12) as shown in Figures 11(a), 11(b), 11(c), 11(d), 11(e) and (11f) precipitated along grain boundaries. The grain size of the base metal was approximately 200 μm . These figures show the microstructure of an FSP-treated sample of the same RD without coolant.

Figure 9 optical microscopy images of the cross-sectional view of the AZ31/AZ91 mating after FSW appeared. Under this distribution of β phase (Mg17Al12) is restricted at the receding way (AZ91-Mg way). The nuzzetet zones we usually discovered to be mixing with both AZ31/AZ91 Mg alloys, here the distribution of AZ31 alloy also appeared to be greater than that of AZ91 alloy. This is evident from the more ductile nature of AZ31 compared to AZ91 alloy. This area indicated by the white arrow in Figure 10 appears perfect metallurgical continuous between AZ31/AZ91-Mg alloys. On this left for the interface, the β -(Mg17Al12) phase [37-39] appeared as small discrete white colour atoms. Compared with the original microstructural for Mg-based alloy AZ91 in Figure 11(a), it is assumed that the network-like Mg17Al12 phase at grain boundaries was decomposed into low-size grains under FSW.



Fig. 9 Micro structure taken at a cross-section of welding process at low magnification dissimilar welding process Az-91/Az-31



Fig. 10 Micro structure taken at the cross-section of welding process at high magnification dissimilar welding process Az-91/Az-31

3.4. Optical Microscope at Dissimilar AZ91/Az31 Cross Sectional View

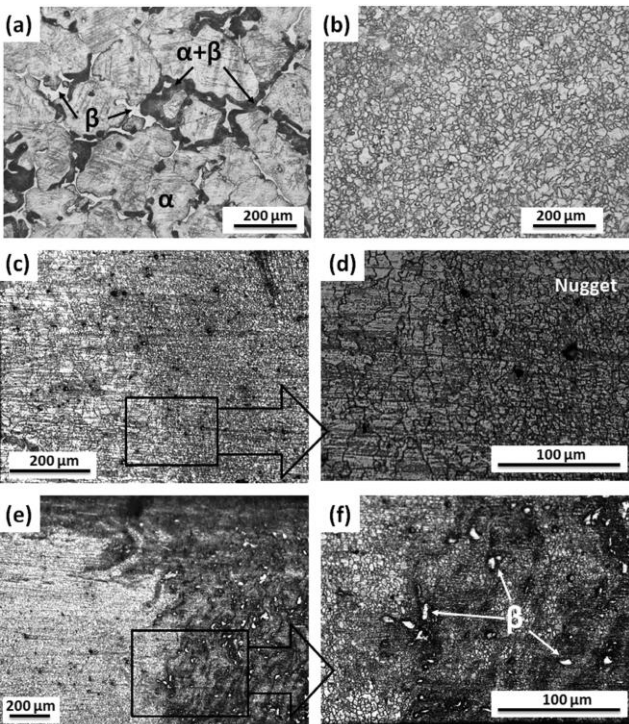


Fig. 11 Optical microscope collected the pictures from different regions 11a. Az91-Mg alloy base Microstructure, 11b. Az-31 base metal micro-structure, 11c. Nugget zone also for base metal interface, at AZ31-M composition, 11d. Under this enlarged picture, 11e. Nugget zone for a base metal interface on AZ91 alloy side, 11f. Enlarged image for Az91

Figure (11a) also shows the distribution of the ‘ $\alpha+\beta$ ’ area under the ‘ α ’ (Mg/Al for med crystal solution) under the ‘ β ’ regions (Mg/Al compound, Mg₁₇Al₁₂). This region indicates for the black arrow in Figure 10 contains more fine-grained AZ91-Mg alloy compared to AZ31-Mg alloy. This means that these regions are enriched in aluminum compared to other bright regions in the nugget zone (less AZ91 present). Therefore, it can be confirmed that the AZ31 region and the mixed region of AZ31/AZ91 are mixed in the nugget region. This observation also suggests an increased aluminum solubility under the nuzzet zone, which appropriately affects the bulk mechanical properties of the compound.

3.4.1. Similar butt Joint with Metal Process Parameters (AZ-91/31)/ 50 Tool Traverse Speed (TTS)

In AZ31/AZ91 Dissimilar butt welding at 50 tool traverse speed, the weld was made at different RPMs, here as per my experimental work we used here CNC-vertical milling machine, and a tool was tapered threaded at a 4.3mm length will go between the two metals and the width will be at the top point that is tool shoulder the width of butt weld is 5mm and the depth point bottom [37] it touches with 2mm tip and the shoulder to endpoint the length was 4.3mm but here we use the material thickness was 6.1 to 6.3mm because we need to achieve the proper welding.

FSW is currently used to successfully consolidate in Figures 12(a), 12(b) and 12(c), sheets of AZ91 Mg alloy and AZ31 alloy. Achieving a robust weld between two dissimilar metals has been found to be highly dependent on speed. We found that the bonding between AZ91-Mg and AZ31 alloys is often the result of mechanical intermixing and weak metallurgical bonding.

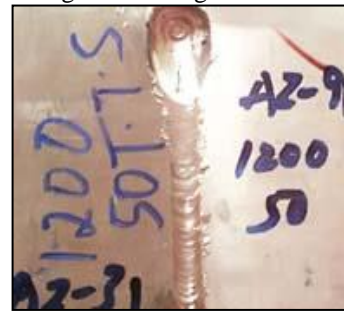


Fig. 12a The weld was made at 1200rpm at 50 tool traverse speed with dissimilar welding Az91/Az31 alloy



Fig. 12b The weld was made at 1400rpm at 50 tool traverse speed with dissimilar welding Az91/Az31 alloy

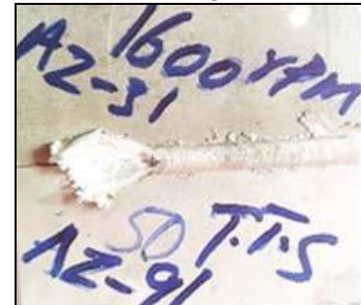


Fig. 12c The weld was made at 1600rpm at 50 tool traverse speed with dissimilar welding Az91/Az31 alloy

The stirred quarter region and the AZ91 matrix had a sharp interface according to microstructural observations and microhardness studies. Furthermore, it was found that the second phase of AZ91-Mg alloy faded and the particles

Table. 3 Machining process and its defects

S. No	Similar/ Dissimilar (Az31-Az91)	Speed (rpm)	Feed mm/ min	End Results
1	Az(31/31)	1200	25	Good joint without cracks or no defects
2	Az(31/31)	1200	50	Good Sound joint without any cracks or no defects
3	Az(31/31)	1400	25	Sound weld with no defects without cracks
4	Az(31/31)	1400	50	Sound weld with no defects without cracks
5	Az(31/31)	1600	25	Sound weld with no defects without cracks but at the endpoint. It forms contour holes removing material from the workpiece and then it sticks to the tooltip and shoulder less in 25mm TTS
6	Az(31/31)	1600	50	Sound weld with no defects without cracks but at the endpoint, it forms contour holes removing material from the workpiece, and then it sticks to the tooltip and shoulder high in 50mm TTS
7	Az(91/91)	1200	25	Sound joint without cracks or defects
8	Az(91/91)	1200	50	Sound weld with no defects without cracks but at the endpoint, it forms contour holes removing material from the workpiece and then it sticks to the tooltip and shoulder high in 50mm that the center of the process
9	Az(91/91)	1400	25	The Sound joint was made without any cracks or no defects
10	Az(91/91)	1400	50	The Sound joint was made without any cracks or no defects
11	Az(91/91)	1600	25	Sound joint without cracks or defects
12	Az(91/91)	1600	50	The Sound joint was made without any cracks or no defects
13	Az(31/91)	1200	25	The Sound joint was made without any cracks or no defects
14	Az(31/91)	1200	50	From the start to the end of the process it forms very bad welding, it forms hot cracks and improper welding
15	Az(31/91)	1400	25	Not Found
16	Az(31/91)	1400	50	Defects found not a sound weld but it forms hot cracks and also forms counters on the workpiece
17	Az(31/91)	1600	25	Defects found not a sound weld but it forms hot cracks and also forms counters on the workpiece
18	Az(31/91)	1600	50	Defects found not a sound weld but it forms hot cracks and also forms counters on the workpiece

3.6. XRD for AZ31/AZ91 Alloys

The experimental science known as X-ray crystallography uses incident X-rays to bend them in several different directions to determine the atomic and molecular structure of crystals. A picture of the electron density in the crystal can be constructed in three dimensions by measuring the angles and intensities of these diffraction beams as shown in Figure 13. From this electron density, the average positions of atoms in the crystal, their chemical bonding, their crystallographic disorder, and other details can be derived.

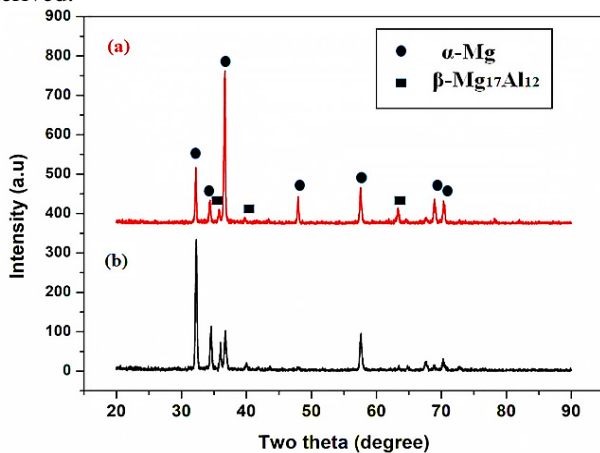


Fig. 13 XRD for Az-31 and Az-91 alloys

3.7. Micro Vickers Hardness Test

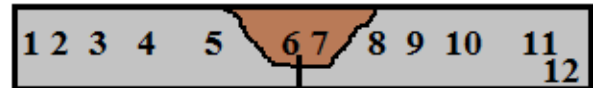


Fig. 14 Micro vicker's hardness test

Figure 14 shows an image of a weld taken with different processing settings. It provides an overview of post-weld observations. From this result, it is clear how important the rotation speed and running speed of the device are to create an impressive intersection. It was found that when the tool was rotated at 1600rpm per minute, additional heat was generated, washing away excess tissue and depositing some ground tissue on the shoulder of the FSW device. Tissue slippage is reported to be exacerbated at feed rates above 25 mm/min, resulting in deep grooves at the junction, as seen in Figure 10. The same behavior was observed in the weld when the device rotation speed was reduced to 1400rpm with a feed of 50mm/min. Similar behavior is observed in welds, where the seam is invisible at the rate of 6mms/min. Curiously, a feed rate of 25mm/min produces a moderately high-quality effect, as shown in Figure 11. During welding, the weld became visible, demonstrating tremendous metallurgical power. Although a genuine joint, failure identified as a hot crack, shown in Figure 10, occurred while the weld joint was periodically cooled to ambient temperature.

Table. 4 Micro vickers hardness values for dissimilar magnesium alloys Az-91/Az-31

Sl. No	Locations	H.V @ 0.5 Kgf Load
1	Parent metal	48.8
2	Parent Metal with near HAZ-1	59.8
3	Parent Metal with near HAZ-2	58.9
4	Parent Metal with near HAZ-3	69.4
5	HAZ	104.9
6	Weld Zone	107.2
7	Weld Zone	110.3
8	HAZ	64.2
9	Parent Metal with near HAZ-1	63.0
10	Parent Metal with near HAZ-2	63.6
11	Parent Metal with near HAZ-3	65.2
12	Parent metal	68.7

The joint appeared to develop similarly while the process continued at 1200rpm and 25mm/min. As earlier as the mate warmed up to room atmospheric condition, the narrow hot cracks were found, same at the weld moving at 1400rpm and 50 mm/min. Fusion welding techniques result from hot cracking during and immediately after solidification. The shrinkage that occurs at some point in the solidification of the liquid metal in the weld explodes the residual stresses in the weld, and if these stresses are large fracture occurs. When these stresses become large or uneven, joints and fractures occur.

The heat generated at the connection point must be dissipated with the FSW through the workpiece, the FSW device, and the surrounding air during heavy rain welding. Much of the heat dissipation in this process was through the tool and workpiece. As a result, different regions of treated and untreated tissue have different temperatures. The thermal conductivity of floor coverings is a valid reason for the formation of hidden stresses. Differences in thermal conductivity at the weld point make it difficult to find residual marks in the presence of contrasting base metals, as in modern tests, and promote hot crack formation after cooling.

Formation of hot fractures during cooling of the joint. This caused the joint, which appeared perfect during manipulation but was inappropriate up to normal atmospheric conditions [39], to magnify the warm fracture as shown in Figures 2(d) and 2(e). As shown in Figure 2(f), at a given feed speed of 25mm/min at 1100rpm, the final heat and flow following the fabric eliminated the formation of thermal cracks and produced disease-free joints. The weld joint goes segment was achieved at 1100rpm with 25mm/min. within the enlarged photo in Figure 3(e), primary materials and a subsequent section with elongated grains are seen.

On the stirring quarter, it became seen that the fabric from Al-6063 had routinely mixed with AZ91 and formed a junction. Pictures were captured by using optical microscopes of basic AZ31 and matching base and stir area interfaces, in addition to base AZ91. The microstructure of

the bottom and stir region are compared in Figure 5 subsequent to the AZ91 Mg alloy.

In advance than FSW in Figure 5(a), the grains incorporate much less than 1% (as seen with the aid of the black arrows). metal aluminium. As visible using the white, an excessive amount of aluminium leads to the formation of community-formed Mg₁₇Al₁₂.arrows. It's interesting to look at how little secondary section is present within the stir sector in contrast to the simple fabric, AZ91 Mg alloy (a hundred and sixty.2 mm) in grain size. Likewise, the grain size turned into decided. AZ31 stir region has a grain size of 17microns, that's much less than the cloth's initial grain size of 94microns [49]. The XRD patterns of the two fundamental materials are shown in parent 6 in Figure 13. The weld joint and so forth XRD plots of the primary substances, with the aid of evaluating all peaks, were found and listed. Trendy statistics (for Al-JCPDS and Mg-JCPDS No 35-0821 respectively).

The X-Ray diffracted of the mating revealed peaks that were indicative of both base substances. Join the welding sector, extra peaks had been discovered, however, following FSW, peak intensities were seen to have risen. Particularly, the strength of (002). Large grain in Figure 5(b) compared to the AZ91 Mg alloy base fabric, size (11.4 microns) grain diameter (160.2 mm). Similarly to that, the grain length was decided as 17microns in the Al-6063 stir sector, that's smaller than the material's preliminary grain size of ninety-four. Each of the premise substances' XRD patterns is displayed in parent 6. Likewise, the weld junction the usage of the simple cloth XRD graphs, by comparing with each peak became recognized and catalogued as general information (for Al-JCPDS and Mg-JCPDS No 35-0821 No 04-0787).

Peaks that correspond to each base substance may be seen in the weld joint's XRD consequences. Inside the weld region, there have been a few new peaks had been discovered, however following FSW, the height intensities were seen to have risen. In particular, the degree of (002), materials for bases that drastically decorate the mechanical corrosion styles, etc. In standard, XRD analysis helps the material from each base material is a gift within the weld area and shows that the most effective orientation occurs there because of FSW.

The joint's microhardness distribution is displayed in Figure 7. Due to the existence of zones, the hardness fluctuations in AZ91 Mg alloy are usually noticed as greater sable combinations of magnesium and aluminium, as well as magnesium and Al (Mg₁₇Al₁₂). The variety of hardness, consequently, ranged from lower on the grains and higher in the presence of the second segment as discovered in our prior research, near the grain border. It's interesting to notice that within the modern study, the stirred area shows much less variation within the substances for bases that considerably decorate the mechanical corrosion styles, and so forth. In general, XRD evaluation helps the material from

each base the raw was present at and shows that was most beneficial orientation occurs there owing to FSW.

Additional studies on overall mechanical performance and corrosion. The microhardness value obtained by measuring the entire weld is displayed. These results show that the hardness gradually increases from AZ31 to AZ91. Large variations in hardness values were found within the nugget zone due to the combined effects of the fine grain structure and the presence of the hard Mg17Al12 phase along with some regions of AZ31. Solid solution strengthening also helps increase the hardness as more aluminum dissolves through the reduced Mg17Al12 phase and the nugget zone becomes a supersaturated solid solution. Therefore, in this study, we successfully demonstrated the feasibility of FSW for joining dissimilar metals, especially difficult-to-join metals such as Mg alloys (AZ31/AZ91), and found that the speed and feed of the effect on hot crack removal were also revealed.

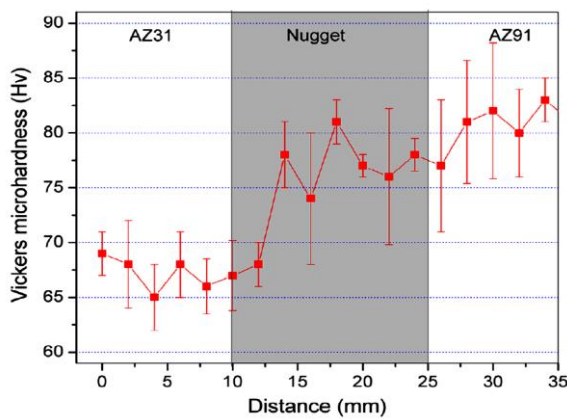


Fig. 15 Micro vickers hardness dissimilar magnesium alloys graph

Figure 15 shows the typical photographs of AZ31/AZ91 welded tensile specimens. Observation shows that the joint strength is higher than that of AZ91 base metal and lower than that of AZ31. This difference was seen at $p < 0.05$ level. The decrease in joint strength can be attributed to the presence of both brittle [35] and soft phases in the joint. These preliminary results, therefore indicate that various Mg alloys are self-bondable by solid-state FSP and the mechanical properties of welded joints are promising. Further studies are planned to evaluate joint performance under different mechanical loads and environmental conditions.

Table. 7 Stress-strain relation for tensile test

S. No	Material	Ultimate Tensile strength (MPa)	Young's Modulus (Mpa)	% of Elongation
1	Az31/Az31 alloy	232 ±6	202±4	15.3±1.2
2	Az91/Az91 alloy	199±3	185±7	4.3±0.3
3	Az31/Az91 alloy	192±2	180±3	4.5±2.2

3.8. Tensile Test Elongation Results

Tensile test of AZ31/ AZ91 alloys and AZ31/AZ91 welded joints (all mean differences were found to be statistically appropriate at a significance level of $p < 0.05$).

3.9. Salt Spray Test on AZ91 and Az31 Alloy

Samples are polished on all surfaces to remove surface defects such as pits and cracks. The sample is polished to reduce the sizscratchmber of scratch lines like at the sample. The initial weight of the sample is observed. Fill a 1 litter beaker with distilled water and mix 35g of He NaCl powder to make a 3.5% NaCl solution. He transfers the prepared solution into two Erlenmeyer flasks. Specimens of each casting type are tied to a wooden rod with a thread so that when the specimen hangs from the neck of the flask it remains completely submerged in the solution without touching the bottom. Cover the flask with aluminum foil and let stand for 24 hours. The sample is then removed, washed with distilled water dried, and weighed. Soak these samples in a chromium trioxide solution for 10 minutes to remove the corrosion products.

The sample is washed again with distilled water and weighed after drying. In die-casting applications, high-purity AZ91 alloy has been shown to produce parts with saltwater corrosion properties that are 10 to 100 times better than standard purity alloy. In the work presented, two major issues for further development of the alloy were resolved. Differences in iron impurity content and activity are quantitatively related to the amount of manganese present in the metal, casting alloys with well-controlled manganese content, and permanent form of sand impurities has been shown to produce parts with saltwater corrosion behavior. Equivalent to die-cast parts. Only the nickel resistance of the alloy was significantly affected by the associated slow solidifies spray rate. Salt spray test on AZ31 Alloy. Corrosion resistance and adhesion of AZ31 magnesium alloy rolled sheet coated with hydroxyapatite (HAp) were evaluated by salt spray test (SST: JIS Z 2371) [22] and cross-cut test (CCT: JIS K 5600).

The duration of HAp coating solution treatment was 4 or 6 hours. Consisting of a continuous inner layer and a porous outer layer, the HAp coating covers the surface uniformly regardless of treatment time. After 7 days of SST, the HAp-coated surface showed no significant delamination, but some visible pits. His HAp coating in non-corrosive areas retained its original morphology after He SST in SEM observations. The Rating Number (RN) of HAp-coated samples was >9 . This was much higher than the RN4 observed in the chemically polished sample almost completely covered with fusion from corrosion. The RN of HAp-coated samples increased slightly with longer treatment times. The adhesion of HAp coatings was not affected by SST according to CCT. After removing the corrosion products and HAp coating from the uncorroded areas, small holes of several hundred microns in diameter appeared. However, no blanket corrosion occurred under the HAp coating. HAp coatings exhibit high corrosion resistance and good adhesion to AZ31 substrates.

3.10. SEM Analysis

This SEM image of the crack surface of the tensile test piece is shown a fracture forming in heat affected zone of the FSW bonding process.

Microphotographs show a small brittle surface morphology on the fracture surface in Figures 16(a) and (b). The macro chart also shows large sink marks. This may indicate a casting defect.

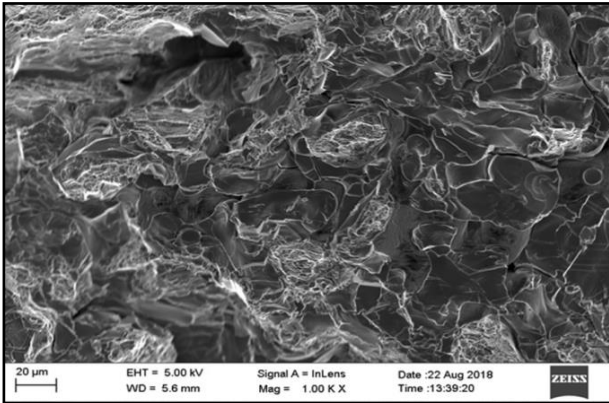


Fig. 16a SEM picture for high magnification to find how the material behavior and contains the microstructure of AZ91 alloy contains for the intermetallic structure of Al-Sm (Al₂Sm /Al₁₁Sm₃) and Al-Mn-Sm, α -Mg and β -Mg₁₇Al₁₂ phase

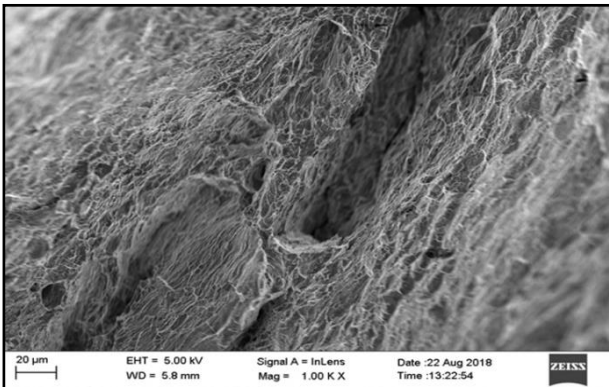


Fig. 16b SEM picture for high magnification to find how the material behavior and it contains the (Al₂Sm and Al₁₁Sm₃) and Al-Mn-Sm, α -Mg and β -Mg₁₇Al₁₂ phase and shows the fracture surface and how the garins activities (medium magnification)

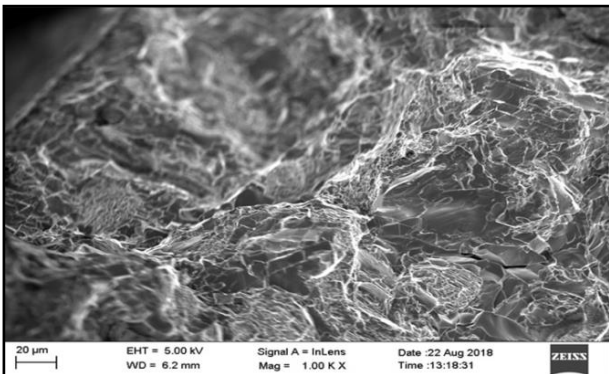


Fig. 16c SEM show high magnification of the grains having what kind of alloys is forming under Al-Mn-Sm, α -Mg and β -Mg₁₇Al₁₂ phase

Two macro images covered the entire fracture surface. The magnification of SEM is 1500x. The fracture surface field is shown at 1500x magnification. A trough-like surface that may have been caused by casting errors has been corrected at high magnification.

This image is the same sample, but with a different fracture surface. You can see the fine morphology of the fracture surface at a high magnification of 1500 times. This SEM image shows a magnified image of 1500 times. The cracked surface forms thin cracks running perpendicular to the stress paths. In the heat-affected zone, fractures appear as intergranular cracks running along the direction of grain movement. Figure 16(c) shows the central 1500X SEM picture of the material at the fracture area. This fracture era is brittle, the fracture surface is fine-grained, and there is no pitting corrosion. It shows a fracture surface area containing a large trough that may indicate a fault at the material surface. The huge valley that appeared on the fracture surface was resolved at 1500x magnification. Figure 12 shows another fracture patch with deep grooves in the sample fracture material.

4. Conclusion

Friction stir welding is currently used to successfully consolidate sheets of AZ91 Mg alloy and AZ31 Mg alloy. Achieving a robust weld between two dissimilar metals has been found to be highly dependent on the speed of rotation and travel of the tool. A tool rotation speed of 1100rpm and a tool travel speed of 25mm/min were determined to be suitable settings for an FSW fixture with a shoulder diameter of 15mm, a conical pin of 3-1mm, and a length of 3mm. We found that the bonding between AZ91-Mg and AZ31-Mg alloys is often the result of mechanical intermixing and weak metallurgical bonding.

The stirred quarter region and the Al-6063 matrix had a sharp interface according to microstructural observations and microhardness studies. Furthermore, it was found that the second phase of AZ91-Mg alloy faded and the particles of the stirrer became smaller. No significant new values were found in the XRD analysis after FSW.

Initial results suggest similar studies to determine the effects of the presence of various metals in welded joints on the mechanical and corrosive behavior of the joints. Using AZ91 Mg FSW and additional studies on mechanical performance, corrosion range and AZ-31 base fabric, it is clear that the alloy and Al6063 alloy sheets can be joined. Moreover, it was noted that the second segment of AZ91-Mg alloy with smaller grains decreased in the stir region. No significant new values were found in the XRD analysis after FSW.

Additional research is to determine the impact of using non-identical metals. It is proposed to evaluate how the presence of dissimilar metals in the welded joint affects the mechanical and corrosion properties of the joint.

References

- [1] B. L. Mordike and T. Ebert, "Structural Materials: Properties, Microstructure and Processing," *Materials Science and Engineering: A*, vol. 302, pp. 37-45, 2001.
- [2] S. Nallusamy, "Analysis of Welding Properties in FSW Aluminium 6351 Alloy Plates Added with Silicon Carbide Particles," *International Journal of Engineering Research in Africa*, vol. 21, pp. 110-117, 2016. Crossref, <https://doi.org/10.4028/www.scientific.net/JERA.21.110>
- [3] H. E. Fridrich and B. L. Mordike, "Magnesium Technology," *Springer, Germany*, 2006. Crossref, <https://doi.org/10.1007/3-540-30812-1>
- [4] Frank Czerwinski, "Welding and Joining of Magnesium Alloys," In book: *Magnesium Alloys - Design, Processing and Properties*, 2011. Crossref, <https://doi.org/10.5772/560>
- [5] R.S. Mishra and Z.Y. Ma, "Friction Stir Welding and Processing," *Materials Science and Engineering: R: Reports*, vol. 50, no. 1-2, pp. 1-78, 2005. Crossref, <https://doi.org/10.1016/j.mser.2005.07.001>
- [6] R. S. Mishra, P. S. De and N. Kumar, "Fundamentals of the Friction Stir Process. In: Friction Stir Welding and Processing. Springer, Cham. Crossref, https://doi.org/10.1007/978-3-319-07043-8_2
- [7] A. C. Somasekharan and L. E. Murr, "Microstructures in Friction-Stir Welded Dissimilar Magnesium Alloys and Magnesium Alloys to 6061-T6 Aluminum Alloy," *Materials Characterization*, vol. 52, no. 1, pp. 49-64, 2004. Crossref, <https://doi.org/10.1016/j.matchar.2004.03.005>
- [8] C.Y. Lee, W.B. Lee, Y.M. Yeon and S.B. Jung, "Friction Stir Welding of Dissimilar Formed Mg Alloys (AZ31/AZ-91)," *Materials Science Forum*, vol. 486-487, pp. 249-252, 2005. Crossref, <https://doi.org/10.4028/www.scientific.net/MSF.486-487.249>
- [9] "ASTM E8/E8M-11, Standard Test Methods for Tension Testing of Metallic Materials," *ASTM International*, 2009. Crossref, https://doi.org/10.1520/E0008_E0008M-11
- [10] R. W. Messler, "Principles of Welding: Processes, Physics, Chemistry and Metallurgy," *Wiley India Pvt. Ltd*, New Delhi, 2004.
- [11] R. S. Parmar, "Welding Engineering and Technology," 2nd Ed, *Khanna Publishers*, 2013.
- [12] B. Ratna Sunil, G. Pradeep Kumar Reddy, A. S. N. Mounika, P. Navya Sree, P. Rama Pinneswari, I. Ambica, R. Ajay Babu and P. Amarnadh, "Joining of AZ31 and AZ-91 Mg Alloys by Friction Stir Welding," *Journal of Magnesium and Alloys*, vol. 3, no. 4, pp. 330-334, 2015. Crossref, <https://doi.org/10.1016/j.jma.2015.10.002>
- [13] Prakash Kumar Sahu and Sukhomay Pal, "Multi Response Optimization of Process Parameters in Friction Stir Welded AM20 Mg Alloy by Taguchi Grey Relational Analysis," *Journal of Magnesium and Alloys*, vol. 3, no. 1, pp. 36-46, 2015. Crossref, <https://doi.org/10.1016/j.jma.2014.12.002>
- [14] V. Jaiganesh and P. Sevvell, "Effect of Process Parameters on the Microstructural Characteristics and Mechanical Properties of AZ80A Mg Alloy During Friction Stir Welding," *Transactions of the Indian Institute of Metals*, vol. 68, pp. 99-104, 2015. Crossref, <https://doi.org/10.1007/s12666-015-0620-y>
- [15] Bhukya Srinivasa Naik, Xinjin Cao, Priti Wanjara, Jacob Friedman and Daolun Chen, "Residual Stresses and Tensile Properties of Friction Stir Welded AZ31B-H24 Mg Alloy in Lap Configuration," *Metallurgical and Materials Transactions B*, vol. 46, no. 4, pp. 1626-1637, 2015. Ceossref, <https://doi.org/10.1007/s11663-015-0338-6>
- [16] S. Mironov, "Microstructure Evolution during Friction Stir Welding of AZ31 magnesium Alloy," *Acta Materialia*, vol. 100, pp. 301- 312, 2015. Crossref, <https://doi.org/10.1016/j.actamat.2015.08.066>
- [17] P. Sevvell and V. Jaiganesh, "Characterization of Mechanical Properties and Microstructural Analysis of Friction Stir Welded AZ31B Mg Alloy through Optimized Process Parameters," *Procedia Engineering*, vol. 97, pp. 741-751, 2014. Crossref, <https://doi.org/10.1016/j.proeng.2014.12.304>
- [18] Srinivasa Naik Bhukya, Daolun Chen, Xinjin Cao and P. Wanjara "Texture Development in a Friction Stir Lap Welded AZ1B Mg Alloy," *Metallurgical and Materials Transactions A*, vol. 45, no. 10, pp. 4333-4349, 2014. Crossref, <https://doi.org/10.1007/s11661-014-2372-4>
- [19] Yong Zhao, Qingzhao Wang, Xudan He, Jian Huang, Keng Yan and Jie Dong, "Microstructure and Mechanical Properties of Friction Stir Welded MG2Nd- 0.3Zn-0.4Zr Mg Alloy," *Journal of Materials Engineering and Performance*, vol. 23, pp. 4136-4142, 2014. Crossref, <https://doi.org/10.1007/s11665-014-1173-7>
- [20] S. Ugender, A. somi Reddy and A. Kumar, "Microstructure and Mechanical Properties of AZ31B Mg Alloy by Friction Stir Welding," *Procedia Material Science*, vol. 6, pp. 1600-1609, 2014. Crossref, <https://doi.org/10.1016/j.mspro.2014.07.143>
- [21] Inderjeet Singh, Gurmeet Singh Cheema and Amardeep Singh Kang, "An Experimental Approach to Study the Effect of Welding Parameters on Similar Friction Stir Welded Joints of AZ31B-O Mg," *Procedia Engineering*, vol. 97, pp. 837-846, 2014. Crossref, <https://doi.org/10.1016/j.proeng.2014.12.358>
- [22] S. Rajakumar, V. Balasubramanian and A. Razalrose, "Friction Stir Welding of AZ61A Mg Alloy," *The International Journal of Advanced Manufacturing Technology*, vol. 68, pp. 277-292, 2013. Crossref, <https://doi.org/10.1007/s00170-013-4728-0>
- [23] Santhosh V and Natarajan U, "Evaluation of Temperature Distribution of Solid State Welded AA6061Alloy," *SSRG International Journal of Mechanical Engineering*, vol. 6, no. 2, pp. 13-16, 2019. Crossref, <https://doi.org/10.14445/23488360/IJME-V6I2P103>
- [24] A. Razal Rose, V. Balasubramanian and K. Manisekar, "Influences of Welding Speed on Tensile Properties of Friction Stir Welded AZ61A Magnesium alloy," *Journal of Materials Engineering and Performance*, vol. 21, no. 2, pp. 257-265, 2012. Crossref, <https://doi.org/10.1007/s11665-011-9889-0>

- [25] K. L. Harikrishna, J. J. S. Dilip, K. Ramaswamy Choudary, V. V. Subba Rao, S. R. Koteswara Rao, G. D. Janaki Ram, N. Sridhar and G. Madhusudhan Reddy, "Friction Stir Welding of Mg Alloy ZM21," *Transactions of the Indian Institute of Metals*, vol. 63, pp. 807-811, 2010. Crossref, <https://doi.org/10.1007/s12666-010-0123-9>
- [26] Raju Kamminana and Venkatasubbaiah Kambagowni, "Modeling and Optimization of Process Parameters of Friction Stir Welding of Al-Li Alloy AA2050 by Response Surface Methodology," *SSRG International Journal of Engineering Trends and Technology*, vol. 69, no. 5, pp. 208-227, 2021. Crossref, <https://doi.org/10.14445/22315381/IJETT-V69I5P228>
- [27] M. R. Pishevar, J. Aghazadeh Mohandesi, H. Omidvar and M. A. Safarkhanian, "Influences of Friction Stir Welding Parameters on Microstructural and Mechanical Properties of AA5456 (Almg5) at Different Lap Joint Thicknesses," *Journal of Materials Engineering and Performance*, vol. 24, pp. 3835-3844, 2015. Crossref, <https://doi.org/10.1007/s11665-015-1683-y>
- [28] Nallusamy, S and Karthikeyan, A., "Synthesis and Wear Characterization of Reinforced Glass Fiber Polymer Composites with Epoxy Resin Using Granite Powder," *Journal of Nano Research*, vol. 49, no. 1, pp. 1-9, 2017. Crossref, <https://doi.org/10.4028/www.scientific.net/JNanoR.49.1>
- [29] A. Kouadrihenni and Laurent Barrallier, "Mechanical Properties, Microstructure and Crystallographic Texture of Magnesium AZ-91-D Alloy Welded by Friction Stir Welding," *Metallurgical and Materials Transactions A*, vol. 45, pp. 4983-4996, 2014. Crossref, <https://doi.org/10.1007/s11661-014-2381-3>
- [30] P. Sevvel and V. Jaiganesh, "Characterization of Mechanical Properties and Microstructural Analysis of Friction Stir Welded AZ31B Mg Alloy through Optimized Process Parameters," *Procedia Engineering*, vol. 97, no. 741-751, 2014. Crossref, <https://doi.org/10.1016/j.proeng.2014.12.304>
- [31] J. Yang, D. R. Ni, D. Wang, B. L. Xiao and Z. Y. Ma, "Strain Controlled Low Cycle Fatigue Behavior of Friction Stir Welded AZ31 Magnesium Alloy," *Metallurgical and Materials Transactions A*, vol. 45, pp. 2101-2115, 2014. Crossref, <https://doi.org/10.1007/s11661-013-2129-5>
- [32] J. Yang, D. Wang, B. L. Xiao, D. R. Ni and Z. Y. Ma, "Effects of Rotation Rates on Microstructure, Mechanical Properties and Fracture Behavior of Friction Stir Welded (FSW) AZ31 Magnesium Alloy," *Metallurgical and Materials Transactions A*, vol. 44, pp. 517-530, 2013. Crossref, <https://doi.org/10.1007/s11661-012-1373-4>
- [33] Lechoslaw Tuz, "Friction Stir Welding of AZ-91 and AM Lite Magnesium Alloys," *Welding International*, vol. 27, no. 4, pp. 265-267, 2013.
- [34] Nallusamy, S., "A Review on the Effects of Casting Quality, Microstructure and Mechanical Properties of Cast Al-Si-0.3Mg Alloy," *International Journal of Performability Engineering*, vol. 12, no. 2, pp. 143-154, 2016.
- [35] Kazuhiro Nakata, "Friction Stir Welding of Magnesium Alloys," *Welding International*, vol. 23, no. 5, pp. 328-332, 2009. Crossref, <https://doi.org/10.1080/09507110802542668>
- [36] B. Ratna Sunil, G. Pradeep Kumar Reddy, A.S.N. Mounika, P. Navya Sree, P. Rama Pinneswari, I. Ambica, R. Ajay Babu and P. Amarnadh,, "Joining of AZ31 and AZ-91 Mg Alloys by Friction Stir Welding," *Journal of Magnesium and Alloys*, vol. 3, no. 4, pp. 330-334, 2015. Crossref, <https://doi.org/10.1016/j.jma.2015.10.002>
- [37] Juan Chen, Rintaro Ueji and Hidetoshi Fujii, "Double Sided Friction Stir Welding of Magnesium Alloy with Concave-Convex Tools for Texture Control," *Materials and Design*, vol. 76, pp. 1-10, 2015. Crossref, <https://doi.org/10.1016/j.matdes.2015.03.040>
- [38] H.M. Rao, R.I. Rodriguez, J.B. Jordon, M.E. Barkey, Y.B. Guo, H. Badarinarayan and W. Yuan, "Friction Stir Spot Welding of Rare Earth Containing ZEK 100 Magnesium Alloy sheets," *Materials and Design*, vol. 56, pp. 750-754, 2015. Crossref, <https://doi.org/10.1016/j.matdes.2013.12.034>
- [39] A. Dorbane, B. Mansoor, G. Ayoub, V.C. Shunmugasamy and A. Imad,, "Mechanical Microstructural and Fracture Properties of Dissimilar Welds Produced by Friction Stir Welding of AZ31B and Al6061," *Material Science and Engineering*, vol. 651, pp. 720-733, 2016. Crossref, <https://doi.org/10.1016/j.msea.2015.11.019>
- [40] Shailja Mishra, Diyana Patel, Hiten Patel, Smit Patel, Mohit Teacher, "Evaluation of Mechanical Properties for Bi-Metallic Welds," *SSRG International Journal of Mechanical Engineering*, vol. 4, no. 4, pp. 1-4, 2017. Crossref, <https://doi.org/10.14445/23488360/IJME-V4I4P101>
- [41] S. Nallusamy, "Thermal Conductivity Analysis and Characterization of Copper Oxide Nanofluids through Different Techniques," *Journal of Nano Research*, vol. 40, pp. 105-112, 2016. Crossref, <https://doi.org/10.4028/www.scientific.net/JNanoR.40.105>
- [42] S. Malopheyev, S. Mironov, V. Kulitskiy and R. Kaibyshev, "Friction Stir Welding of Ultra Fine Grained Sheets of Al-Mg-Sc-Zr Alloy," *Materials Science and Engineering A*, vol. 624, pp. 132-139, 2015. Crossref, <https://doi.org/10.1016/j.msea.2014.11.079>
- [43] H.M. Rao, B. Ghaffari, W. Yuan, J.B. Jordon and H. Badarinarayan, "Effect of Process Parameters on Microstructure and Mechanical Behaviors of Friction Stir Linear Welded Aluminium to Magnesium," *Material Science and Engineering: A*, vol. 651, pp. 27-36, 2016. Crossref, <https://doi.org/10.1016/j.msea.2015.10.082>
- [44] Banglong Fu, Guoliang Qin, Fei Li, Xiangmeng Meng, Jianzhong Zhang and Chuansong Wu, "Friction Stir Welding Process of Dissimilar Metals of 6061-T6 Aluminum Alloy to AZ31B Magnesium Alloy," *Journal of Material Processing Technology*, vol. 218, pp. 38-47, 2015. Crossref, <https://doi.org/10.1016/j.jmatprotec.2014.11.039>
- [45] Santhosh V, Natarajan U, "Evaluation of Temperature Distribution of Solid State Welded AA6061Alloy," *SSRG International Journal of Mechanical Engineering*, vol. 6, no. 2, pp. 13-16, 2019. Crossref, <https://doi.org/10.14445/23488360/IJME-V6I2P103>

- [46] M. Yugandhar, B. Prabhakar Kammar and S. Nallusamy, "Experimental Study and Analysis of Friction Stir Welding on Az-91Mg Alloy by using SEM," *International Journal of Engineering Trends and Technology*, vol. 70, no. 10, pp. 110-122, 2022. Crossref, <https://doi.org/10.14445/22315381/IJETT-V70I10P213>
- [47] G. Padmanabhan and V. Balasubramanian, "An Experimental Investigation on Friction Stir Welding of AZ31B Magnesium Alloy," *The Journal of Advanced Manufacturing Technology*, vol. 49, pp. 111-121, 2010. Crossref, <https://doi.org/10.1007/s00170-009-2368-1>
- [48] Chowdhury, S.H., Chen, D.L., Bhole, S.D and Xinjin Cao, "Friction Stir Welded AZ31 Magnesium alloy, Microstructure, Texture and Tensile Properties," *Metallurgical and Materials Transactions A*, vol. 44, pp. 323-336, 2013. Crossref, <https://doi.org/10.1007/s11661-012-1382-3>
- [49] R.Z. Xu, D.R. Ni, Q. Yang, C.Z. Liu and Z.Y. Ma, "Pinless Friction Stir Spot Welding of Mg-3Al-1Zn Alloy with Interlayer," *Journal of Material Science and Technology*, vol. 32, no. 1, pp. 76-88, 2016. Crossref, <https://doi.org/10.1016/j.jmst.2015.08.012>